Nationaal Lucht- en Ruimtevaartlaboratorium
National Aerospace Laboratory NLR

NLR TP 97249

Experimental study of the flow around two scaled 3D swept wings

J.H.M. Gooden, C. Gleyzes and Y Maciel

DOCUMENT CONTROL SHEET

	ORIGINATOR'S REF.		SECURITY CLASS.
	NLR TP 97249 U		Unclassified

ORIGINATOR
National Aerospace Laboratory NLR, Amsterdam, The Netherlands

TITLE
Experimental study of the flow around two scaled 3D swept wings

PRESENTED AT
the 28th AIAA Fluid Dynamics Conference held at Snowmass, CO, USA, June 29 - July 2, 1997

AUTHORS	DATE	pp	ref
J.H.M. Gooden, C. Gleyzes and Y Maciel	970507	16	17

DESCRIPTORS

Delta wings	Three dimensional boundary layer
Error analysis	Turbulent boundary layer
Flow measurements	Wakes
Instrument errors	Wind tunnel models
Pressure distribution	Wind tunnel tests
Quality control	Wind tunnel walls

ABSTRACT
The paper describes the results of an extensive experimental investigation of the three-dimensional turbulent boundary-layers on both sides of a swept wing and its wake. Although the experiment was carried out at low speed, the shape of the wing was designed such as to obtain flow conditions resembling those on practical transonic swept wings, with emphasis on the three-dimensionality of the viscous flow. Mean velocity profiles were determined at nearly 300 stations, while full 3D turbulence measurements were executed at over 200 stations. A special and probably unique feature is that a c
omplete independent check was obtained by executing measurements at the same Reynolds number on two scaled test set-ups in two wind tunnels (the ONERA-F2 and the NLR-LST) using a number of different measurement techniques. This fact, together with an extensive error-analysis, has contributed significantly to the reliability of the experimental data and also gives an impression of the uncertainty range of the data. The work was carried out within the GARTEUR framework as a collaborative effort by DERA, DLR, FFA, NLR and ONERA/CERT.

Contents

(16 pages in total)

EXPERIMENTAL STUDY OF THE FLOW AROUND TWO SCALED 3D SWEPT WINGS

J.H.M. Gooden*
National Aerospace Laboratory NLR, postbus 153, 8300 AD Emmeloord, The Netherlands
C. Gleyzes†
ONERA/CERT, bp 4025, 31055 Toulouse Cedex 04. France
Y. Maciel‡
(presently) Laval University, Quebec City, Canada GIK 7P4

Abstract

The paper describes the results of an extensive experimental investigation of the three-dimensional turbulent boundary-layers on both sides of a swept wing and its wake. Although the experiment was carried out at low speed, the shape of the wing was designed such as to obtain flow conditions resembling those on practical transonic swept wings, with emphasis on the three-dimensionality of the viscous flow. Mean velocity profiles were determined at nearly 300 stations, while full 3D turbulence measurements were executed at over 200 stations. A special and probably unique feature is that a complete independent check was obtained by executing measurements at the same Reynolds number on two scaled test set-ups in two wind tunnels (the ONERA-F2 and the NLR-LST) using a number of different measurement techniques. This fact, together with an extensive error-analysis, has contributed significantly to the reliability of the experimental data and also gives an impression of the uncertainty range of the data. The work was carried out within the GARTEUR framework as a collaborative effort by DERA, DLR. FFA. NLR and ONERAKERT.

Introduction

Turbulence modelling still forms an indissoluble part of computational aerodynamics. Computer power is not, and for some time to come will not be, sufficient to calculate flows at flight Reynolds numbers by solving the Navier Stokes equations including the smallest flow length scales. Consequently, turbulence modelling will be required to describe the properties of these small scales, resulting in the Reynolds Averaged Navier Stokes (RANS) approximation. Moreover, the length scales resolved are not small enough yet to allow the use of universally applicable isotropic turbulence models. Therefore. suitable turbulence models are to be devised, that apply to the flow under consideration. This holds especially for 3D flows, as usually occur on the swept wings of airliners. So, there is a strong need for 3D boundary layer and wake data to be able to develop suitable turbulence models.

At present. different experimental datasets on 3D boundary layers exist. These experiments often are simplified 3D cases. General characteristics of these experiments are e.g.:

- mainly crosswise pressure gradient (Rhyming & Truong', Schwarz & Bradshaw[2], Pompeo[3]);
- mainly streamwise pressure gradient (Anderson & Eaton', Flack & Johnston[5], Van den Berg & Elsenaar[6], Bradshaw & Pontikos[7], Baskaran et al.[8]);
- flow driven by changing transverse shear stress (Driver & Hebbar[9]).

Also very few turbulence data are available for 3D wakes. Moreover, the experimental conditions generally are not typical of wing-conditions, due to:

- thick boundary layers, and consequently dominance of pressure gradients on the flow;

* Senior Research Scientist. Aerodynamic Engineering and Aeroelasticity Department (email: gooden@nlr.nl)
† Senior Research Scientist, Aerothermodynamics Department. (email:gleyzes@onecert.fr)
*Professor. Mechanical Engineering Department (email:ymaciel@gmc.ulaval.ca), formerly: ONERAKERT

- rapid downstream changes leading to history effects;
- no typical transonic pressure distribution.

Another important point is that independent checks, material for assessing the accuracy of the data obtained, are rare.

Therefore the need existed to perform an experiment which was tailored more to the needs of aircraft development. Some general characteristics of the experiment designed are:

flow typical for transonic wings, but including an area where the flow is close to separation on the wing suction side;

both boundary layer and wake to be measured;

inflow and outflow boundary conditions to be measured in cross-sections in front of and behind the wing and at the tunnel walls for future calculation purposes;

duplication of measurements on two scaled test set-ups in two geometrically similar wind tunnels (reliability of data);

large model dimension (ease of measurement).

of the key features of this project is the duplication of the test in two wind tunnels. The scale of both test set-ups was different and different measurement techniques were used. The main objective was to produce a reliable database for turbulence model validations in both 3D boundary layers and wakes. To this end much effort was put into a careful error-analysis of the measurement techniques used and the explanation of the (small) differences found between both tunnels. This topic is especially highlighted in this paper.

The experiment was completed in 1995 and generated a large database that will become universally available in some years. In view of the substantial effort involved, it was conducted in the GARTEUR framework. Participating parties were: DERA, DLR, FFA, NLR and ONERA/CERT. Further details on the project, on the model characteristics and initial results can be found in Van den Berg", Firmin and McDonald" and Gleyzes et al[12]. A summary of the resulting data and a comparison between different sets of results will be given in this paper.

Test Set-up

Although airliners usually cruise at transonic speeds, the test was not conducted at transonic but at low speed to keep the measurement constraints at an acceptable level. Nevertheless, conditions typical for a transonic wing were simulated as much as possible. This approach is considered admissible as effects of compressibility on turbulence may be considered sufficiently small at present-day cruise speeds. Finally, the cross-sections of the NLR/LST (presently: DNW/LST) and ONERA/F2 are very nearly to scale allowing a parallel test as desired.

Wing model design

The wing was designed according to the following constraints:

- a pressure distribution like a modern transonic wing with rear-loading;
- flow close to separation on the suction side on the wing outboard part;
- boundary layer on the pressure side getting close to separation as well but relaxing afterwards (rear loading alike);
- significant three-dimensionality and spanwise variation of the flow;
- General wing characteristics should be as follows: 30" sweep, aspect ratio = 1.5, taper ratio = 0.5;
- To obtain large model dimensions and, consequently, thick boundary layers at a reasonable Reynolds-number ($3.3*10^6$), the model was allowed to span 80% of the tunnel largest cross-dimension. This meant that model design had to be done taking into account the wind tunnel wall influence.

The wing design was done by DERA and the initial design was tested with a smaller scale pilot model. From this it appeared that small modifications in the tip and root-area were desirable. The main wing geometry remained unchanged.

Wing model construction

The structural design and manufacture of the final models were done by FFA (composite-sandwich shell structure) and the instrumentation was provided by FFA, DLR and DERA. The models had mean wing chords $\bar{c}$ of 1.6 *m* and 0.96 *m* for the NLR/LST and the ONERA/F2 respectively. They were equipped with an internal traversing mechanism with 12 traversing positions at 20% local chord (C) to enable accurate measurement of the thin boundary layer initial conditions. Moreover, the instrumentation of the LST-model consisted of: 990 (F2: 605) pressure holes of 0.6 *mm* (F2: 0.5 *mm)* inner diameter, 10 (F2: 0) hot-films for regular transition checks, 72 (F2: 30) plugs of 14 *mm* diameter for fitting instrumentation (like hot-films and triangular wall shear stress blocks).

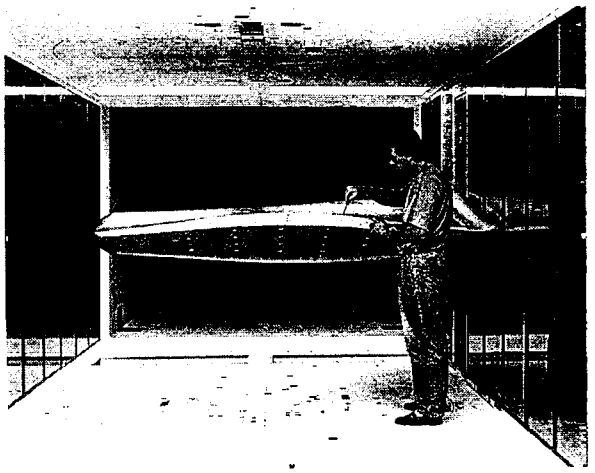

Figure 1. Wing model (mounted upside down) in the NLR/LST

Wind tunnel installation

The models were mounted on the narrowest tunnel wall (to enable the largest wing span), see figure 1. The model incidence was fixed. The transition tripping location was carefully determined to avoid undesired downstream influences on the initial, 20% chord boundary layer. In an early stage, it was hoped to achieve a full turbulent flow by tripping the stagnation line flow. However, due to relaminarization tendencies, this appeared to be unachievable. Therefore, the trips were located at 3% chord suction side and 4% chord pressure side. On the suction side the trip was located upstream of the minimum pressure line. A stainless steel, zigzag trip was used to assure a reliable operation over the entire testing period (several years). Stretched vortical structures behind zigzag trips that sometimes occur in 2D flows were not observed in this 3D boundary layer.

Except at 20% chord, probe traverses were performed by means of slender external traversing mechanisms from the tunnel walls opposite the wing suction and pressure side. Both the LST as well as the F2 mechanism allowed a yawing of the probe into the local flow direction, while the probe incidence remained fixed during the traverse. In view of the flow being partly close to separation, minimum interference was pursued. Additional tests were done to quantify interference effects by comparison with LDA and by using dummy traversing systems. The LDA measurements were done in F2 only, using the rig fixed to this tunnel, enabling three-component, forward and backward scatter measurements.

Tunnel wall pressures were measured in both tunnels by means of removable pressure rails.

Measurement techniques

Boundary layer/wake traverses were performed by LDA and probe-measurements. Probes used with the external traversing system were: p_t-, p_s-, two- and three-hole directional probes, X- and four-hot wire probes. 0.3 *mm* outer diameter pitot-probes or 0.5 *mm* outer diameter Conrad (two-hole) probes were used with the internal traversing system.

Data handling/Error analysis

Total pressures: a turbulence correction was applied to the measured p_t -data using a fit to the measured turbulence data. The measured static pressures were not corrected for turbulence levels as this correction is very uncertain.

X-wire (LST): time-mean voltages and rms-voltages were measured. Velocity data are derived using the effective wire-angle/cosine cooling law concept. At the start of each traverse a two-point in situ velocity calibration is performed (fixing a polynomial describing the relation between hot-wire voltage and effective cooling velocity) which is checked again at the end of the traverse. The full Reynolds-stress tensor is obtained from a combination of 6 rolling angles. A crossflow contamination correction is applied as the mean velocity vector is not always located in the wireplane and locally high turbulence levels exist. Moreover, corrections for gradients (in both mean flow and turbulence quantities) normal to the wire plane are applied according to the simplified relations given in Gooden & Van Lent[13].

An extensive error-analysis was performed on the LST X-wire data, for the effects of two-wire decorrelation and high turbulence levels. Decorrelation may become important in the thinner wing front part boundary layer whereas high turbulence levels occur in the incipient separation region close to the suction side trailing edge. A Monte Carlo technique comparable to the one used by Tagawa, Tsuji & Nagano[14] was used to investigate the errors resulting from both effects. For this purpose artificial (Gaussian) turbulence data including decorrelations between the two wires were generated with the same 3D Reynolds stresses as measured at each point of the traverse (to allow for measurement errors, sensitivity checks were done also with a multiplying factor assigned to these Reynolds stresses). Decorrelation levels were estimated using typical boundary layer integral length scales, depending on the distance to the wall. This study allowed

investigation of both the effects of decorrelation and elevated turbulence levels.

An initial, simplified, analysis of the decorrelation error indicated that:

- the largest error occurs on transverse turbulence intensity, not in shear stresses as far as wireplane quantities are concerned. (Due to tensor-transformations this does not necessarily hold for the flow axis-system!);
- increasing turbulent isotropy leads to reduction of decorrelation errors;
- decorrelation errors are roughly proportional to the square of the probe size.

An example of the full Monte Carlo simulation result is shown in figure 2, showing one case in which decorrelation is dominant (the upper row, corresponding to 60% chord, 68% span, pressure side) and one (the lower row, corresponding to 100% chord, 68% span, suction side) in which high turbulence errors are dominant. The circles indicate the actual flow values as assumed, the drawn line presents the case with zero decorrelation error (zero inter-wire distance) showing the high turbulence level errors only, the dash-dot line shows the results including high turbulence *and* decor-relation effects. Results are valid for the wire-distance of 1.1 *mm* of the actual LST X-wire probe.

The analysis showed that the *maximum* errors due to the combined effects of decorrelation and high turbulence levels for the NLR X-wire data may be expected to be, in: mean velocity: 2%, flow angles: 1°, normal stresses: 5 to 10%, shear stresses: 10 to 20% of the maximum value and turbulent shear direction: 5".

Four-wire (F2): datasampling was used in which the four bridge signals were sampled quasi-simultaneously (within 12 μs). For each measurement point, 4028 samples were obtained during a total sampling time of approximately 20 *s*. An efficient look-up table method is applied, using an inverted directional response diagram. Details are found in Maciel and Gleyzes[15]. The method is especially suited for highly turbulent flows and is based on the decoupling of directional response and velocity magnitude response, thus eliminating the need for an in situ directional response calibration. Gradient corrections for spatial gradients in mean flow and turbulence properties are applied, according to the method of Gooden & Van Lent[13].

The larger probe size of the four-wire probe as compared to the X-wire relative to the model leads to increased decorrelation effects. The relevant dimensions were around 0.3, 0.7 and 1.2 *mm* for the LDA, X-wire (at F2-scale) and four-wire probe, respectively. In some regions (pressure and suction side, $X/C<80\%$) the four-wire probe dimensions probably are close to the limits, especially as far as turbulence data are concerned. Decorrelation errors will be dominant and significant in those regions. Secondly, as the probe acceptance cone limit is found at around 33" off-axis flow angle, significant errors may occur at *local* turbulence intensities exceeding 30%. These levels are found locally (LDA data). To get an idea of the errors occurring due to high turbulence levels, LDA turbulence-data were used as simulated input to the four wire probe data processing method. It appeared that effects are mainly visible on the transverse Reynolds normal stresses and the $\overline{vw}$-shear stress. Other components are not affected.

Still, differences exist between these 'rectified' LDA results and the four-wire probe results as measured. These may be caused partly by interference between the probe-support and the model. Despite an extensive effort to reduce interference as much as possible, residual effects remain in the sensitive, nearly separated region close to the trailing edge. It could be established that probe interference caused flow direction changes near the wall of around 5" in this region for the F2 test set-up and 2" for the LST-test. Outside of the nearly separated region the uncertainties are smaller. Also, this effect seems to cause a slight thinning of the boundary layer, a slight increase in Reynolds normal stresses and a slight decrease in Reynolds shear stresses.

LDA (F2): a 3D, off-axis backscatter (boundary layers) and forward scatter (wake) system was applied. Due to a large off-axis scatter angle, the measurement volume could be considered as almost spherical with a diameter of -0.3 *mm*. A 4 *MHz* frequency shift was applied on each component. Signal processing was done by means of counters, using a 1 μs coincidence window. Seeding (0(1 μm) incense) was introduced downstream of the test section (forward scatter) or just upstream of the settling chamber (backward scatter). Comparison in the near wake showed no difference in results between both ways of seeding. Due to LDA hardware restrictions, the beams were almost normal to the wing surface for the boundary layer measurements, restricting the minimum obtainable distance to the wing surface to around 9 *mm* due to light diffusion on the model surface. Calibration of the beam-directions was done by means of an optical sight.

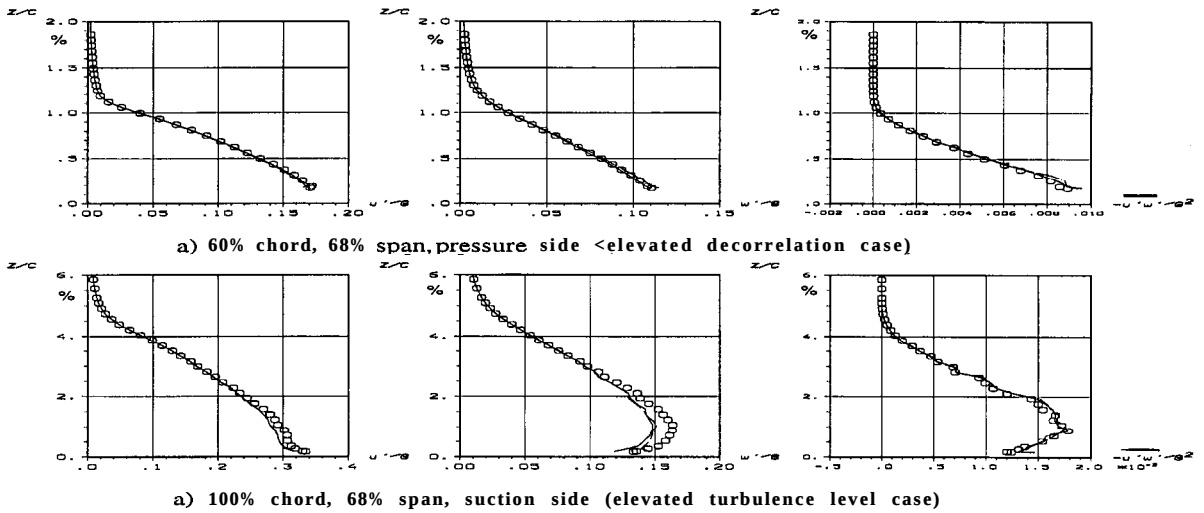

a) 60% chord, 68% span, pressure side <elevated decorrelation case)

a) 100% chord, 68% span, suction side (elevated turbulence level case)

Figure 2. X-wire error analysis: chordwise and wall-normal turbulence intensity, chordwise shear stress (o: actual data, ——: high turbulence level error only, —·—: decorrelation and high turbulence level error)

No large errors were found during a careful assessment of possible bias-errors. 2000 samples per datapoint were taken to obtain a reasonable measurement time, in view of the large number of measurement stations. Unfortunately such a number leads to some scatter in the measured profiles (especially shear stresses).

Finally, measuring low turbulence levels generally is difficult with LDA, due to noise-sources present (Bragg cells, counter resolution, low SNR). This becomes visible if flow turbulence levels are low. In the present test, the main effects occur in the wall-normal turbulence stress close to the edge of the viscous flow region at certain stations.

Hot-films: skin friction direction and magnitude were measured by means of McCroskey (dual, V-type) hot-films. Measurements were performed by DLR and FFA (both in the LST) and ONERA/CERT (F2). Despite the large effort put into the calibration and hot film measurement technique, it appeared very difficult to obtain reproducible results. The vertical orientation of the wing surface in the F2 was especially challenging, due to natural convection flow disturbing the zero wind calibration. This affects chiefly the flow direction measurement. A special technique, using a removable wall jet blowing device, had to be used here. It is estimated that the finally obtained absolute flow angle accuracy is around 3 to 8 degrees and for the wall shear stress magnitude ±10-20%. Note that the repeatability obtained amounts to roughly 1-2%!

Triangular blocks: this method was developed initially by Gaudet et al[16]. It implies an extension of the Stanton tube technique to three dimensions. Equilateral triangular blocks of 0.45 mm thickness are used (figure 3), equipped with 4 pressure holes, one on top, the others halfway the edges (P1 to P4).

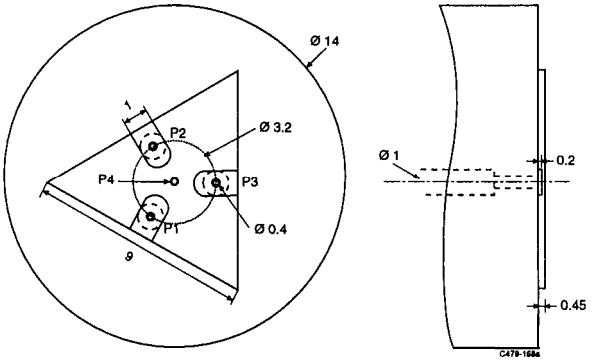

Figure 3. triangular block

Two settings are used for the blocks: 1) with one of the vertices pointing into the flow for measurement of the wall shear-direction, 2) with one side facing the local flow for the shear stress magnitude. There is a drawback to the triangular block technique: like Stanton tubes, the calibration is based on a zero pressure gradient velocity profile. Consequently, uncertainties are introduced in 3D and pressure gradient flows. On the other hand, the reproducibility is excellent, but due to the velocity profile assumptions the estimated

accuracy is around 5" in flow direction and around 10% in wall shear magnitude.

Apart from the two techniques mentioned, skin-friction data were also determined from Clauser-plots and the Preston-tube method (keeping in mind the limitations of the latter methods for use in 3D boundary layers, as these again are based on 2D velocity laws). Finally, skin friction direction was obtained also from extrapolation of the boundary layer profiles.

Global measurement program

The Reynolds number based on the mean chord was kept at a constant value of $3.3*10^6$, resulting in a reference velocity G_0 of around 30 ms^{-1} for the NLR/LST (50 ms^{-1} for the ONERA/F2). Only one configuration was studied, at a fixed angle of attack. At the start of each tunnel-entry about 80 (F2: all) pressures of the pressure distribution were measured again to ensure reproduction of the model conditions. Besides, the turbulent status of the boundary layer was checked using the fixed wall hot films.

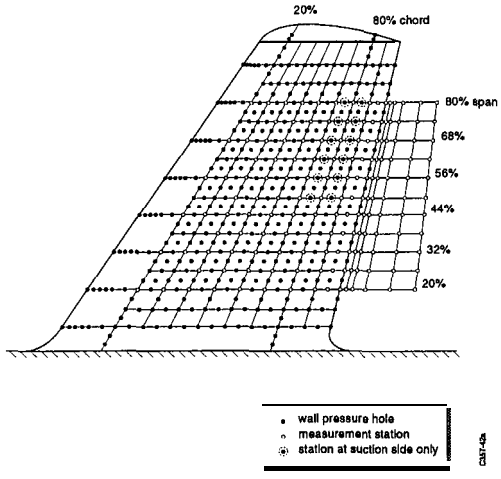

Figure 4. measurement grid

Boundary layer and wake measurements were limited to a domain between 20% and 80% span, and 20% to 130% chord (i.e. on the wing suction and pressure sides). Mean flow data were measured in 11 spanwise sections (-300 stations in total), turbulence data in 6 spanwise sections (-200 stations in total), see figure 4. At a limited number of stations (-50) skin friction measurements were performed using hot-film probes and triangular blocks. The F2 test set-up enabled an extensive use of 3D LDA especially in the very-near and near wake (around 90 stations). In the wake, pressure probe measurements were performed at a number of spanwise stations, while hot-wire probe measurements were only performed at 68% span.

In addition, 3D LDA surveys were performed in the F2 in two planes of the test section, one upstream and one downstream of the model. The static pressure distribution was measured on the four tunnel walls of both tunnels. The model pressure distribution was extensively measured (1000 pressure taps on LST wing, 600 on F2 one).

Discussion of results

Boundary conditions

Boundary conditions needed as input for a variety of CFD methods have been measured. These boundary conditions comprise:

- wing pressure distribution;
- initial conditions: boundary layer profiles at 20% chord;
- boundary layer edge flow angles;
- wind tunnel wall pressure distribution;
- flow conditions at entry plane upstream and exit plane downstream of the model.

The surface pressure distribution and initial line boundary layer profiles were also measured in the pre-test phase to check conformity of both test set-ups. Excellent agreement was found (Gleyzes et al.[12]), see figure 5, showing a comparison between the measured pressure distributions at 56% span.

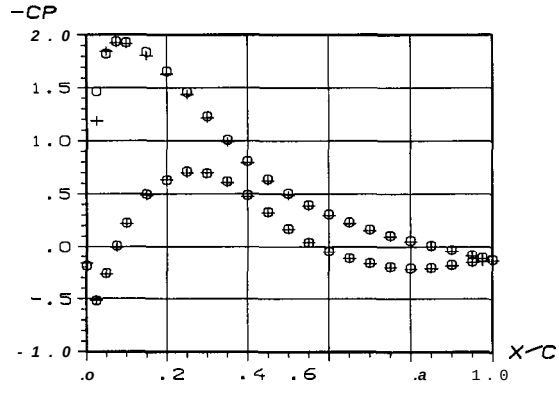

Figure 5. pressure distribution 56% span
(0: LST, +:F2)

Pressure gradients, the actual driving force of the boundary layer, were also compared and show very satisfactory agreement. Boundary layer traverses by

means of the internal traversing mechanism at 20% chord show that edge flow angles are within 0.5" for the two models. Inside the boundary layer (note: thickness only ~0.3% chord, so directional measurement is not straight-forward) differences remain small with a maximum of about 1-2°, mainly in the suction side outboard region.

As additional boundary conditions, the flow conditions at an entry plane upstream, an exit plane downstream of the model and the pressures at the tunnel walls were measured to allow execution of Reynolds Averaged Navier Stokes computations including the wind tunnel walls (without infinitely long test section assumptions). The entry plane is at about 0.4 mean wing chords upstream of the wing apex, the exit plane at about 3 mean wing chords downstream of the wing apex. The mean velocity vector in these planes was determined at 230 points by LDA in the F2. Measurements in the exit plane were supplemented by pitot-probe data to obtain accurate information on the extent of the viscous (p_t-loss) region. Wind tunnel wall static pressures have been measured at 20 circumferential positions over the full test section length in both tunnels.

Wing suction side

The main features of the suction side flow as measured are:

- For X/C > 60% the skin friction is low, especially on the outboard sections, while the flow is close to equilibrium.
- On the last 10% of the chord the adverse pressure gradient increases, leading to a further drop of the skin friction and increasing flow three-dimensionality.
- The chordwise adverse pressure gradient leads to a nearly separated flow close to the outboard trailing edge (shape factor around 2.2, and twist angles greater than 40").

Figure 6 shows the evolution of the velocity magnitude G and crossflow angle β_B-$\beta_{B,e}$ at 68% span. Z_B/C is the dimensionless distance normal to the wall and β_B is the yaw angle measured in the local boundary layer coordinate system (subscript e corresponds to the boundary layer edge).

As far as the comparison between the two tunnels is concerned, it is found that at 20% span the boundary layer on the F2 model on the aft part of the wing is slightly thicker. This presumably is caused by differences in wind tunnel wall boundary layer thickness between LST and F2. Also, in the outboard, incipient separation region, the boundary layer on the F2 model seems to be slightly thicker.

Figure 7 shows results obtained for the chordwise turbulent shear stress $-\overline{u'w'}/G_0^2$. Differences between turbulence data appear to be systematic. Note that these systematic errors could readily be observed, because of the duplicate test! Discrepancies can be seen between the different measurement techniques, caused by the suction side boundary layer being strongly 3D, close to separation and highly turbulent (more than 35% in terms of local turbulence level $\sqrt{\overline{u'^2}+\overline{v'^2}+\overline{w'^2}}/G_0$ in the lower 30% of the boundary layer at the trailing edge). As described above, differences in measured turbulence data not only are due to small differences in flows, but also could be attributed to differences in spatial resolution, elevated turbulence levels and interference effects.

Wing pressure side

On the pressure side, after an initial adverse pressure gradient (between 30 and 70% chord), the rear loading induces a favourable pressure gradient, and makes the boundary layer relax towards a nearly collateral flow. The mean and turbulent flow characteristics at again 68% span are shown in figures 8 and 9.

For all figures, both on the suction and pressure side, the vertical scale has been taken identical, to show the significant difference between the boundary layer thickness on the two sides. As was the case for the suction side, the mean flow results again show excellent agreement both in mean velocity profiles (magnitude) and crossflow angle β_B-$\beta_{B,e}$ not only between the various measurement techniques but also between the two models. Cross-over profiles occur around 40% chord (with small twist angles, however). Maximum twist angles on the pressure side of around 20" are found at 70% chord. At the trailing edge the flow is almost collateral again.

Surface curvature effects are non-negligible at some locations (δ/R around 0.02). A further analysis showed that a simple log law region is no longer present in the velocity profiles (as noted earlier by Barlow & Johnston[17]).

Some differences are seen in the turbulence data (figure 9) however. The boundary layer on the pressure side is thinner than the one on the suction side, increasing the hot-wire decorrelation problems. The shear stresses measured by the four-wire probe in the F2 seem to suffer from this effect (The F2 LDA-data show a closer comparison with the LST X-wire data).

Also at some locations an unlikely large difference in direction between the gradient vector and shear-stress vector measured by the four-wire probe in F2 is observed (not shown here).

Wake

The wake measurement results are shown in figures 10 and 11. The vertical coordinate Z_R is taken relative to the trailing edge position $Z_{R,te}$. β_R is the crossflow angle. It is clear that the wake is strongly 3D, with the external inviscid flow converging on the wing suction side and diverging on the wing pressure side of the wake. At the trailing edge, the mixing of the thick, highly 3D, nearly separated suction side boundary layer, with the thin, nearly 2D pressure side one can be observed. The initial wake shape factors are above 2 in the tip region.

Although the wake is very asymmetric initially, there is a fast recovery to an already fairly symmetric wake at 30% chord downstream of the trailing edge (as far as mean velocities, not turbulent stresses are concerned!). Nevertheless, a significant twist still exists at this position. A general trend is that the relaxation is much more rapid for chordwise quantities than for transversal ones. An interesting feature is that up to 30% downstream of the trailing edge, the wake has moved towards the pressure side, while its thickness is still constant.

The differences in boundary layer thickness between the two models found at 20% span are recognised also in the wake. Likewise, the F2 wake outboard of 68% span perhaps is slightly thicker due to the small differences in the suction side boundary layer.

Turbulence data in the wake show excellent agreement between X- and Four-wire probe and LDA due to the vanishing probe support interference and to an increase in turbulent length scales compared to the boundary layer ones. Figure 11 shows the evolutions of $\sqrt{\overline{v'^2}}/G_0$ (component of velocity fluctuation in the spanwise direction) and $-\overline{u'w'}/G_0^2$ along a normal to the tunnel axis. The relatively large eddy-size in the wake reduces decorrelation errors significantly. Moreover, local turbulence intensities are reduced, although still large, as compared to the wing suction side boundary layer. The correspondence between four-wire data and the other data also shows that the new dataprocessing method, as used for the four-wire probe, is able to give excellent results.

Very few data of 3D asymmetric wakes exist. This experiment thus provides a very useful database for validation of CFD codes for this kind of flows.

Conclusions

The paper presents data obtained in two separate wind tunnels on two identical, but different scale models at equal Reynolds numbers. The flow has been shown to be highly 3D. Mean flow data were obtained at -2.50 stations. Several measurement techniques, including pressure probes, hot-wire probes and LDA were used. Agreement between the mean flow data on the two models, obtained with various measurement techniques is generally highly satisfactory. Differences exist mainly in the incipient separation zones. Turbulence data agree very well in the wake. In some regions differences occur due to either the elevated local turbulence intensities or due to decorrelation effects in hot-wire measurements. The latter affected especially the F2 four-wire data in the thinner pressure side boundary layer. The new four-wire dataprocessing method proved to be accurate and time-efficient.

The experiment highlights the difficulties in measuring turbulent quantities in strongly 3D, highly turbulent flows. In particular, it shows the great importance of duplication to assess the reliability of data. Many turbulence data sets available in literature have been taken without proper independent duplication. The fact that systematic errors can be so significant, as established in this investigation, is reason for some more concern on the confidence level of the experimental Reynolds stress data, currently used by turbulence modellers.

Acknowledgements

The authors wish to acknowledge the contribution of the colleagues of various other institutes to the successful completion of this experiment: NLR (B.van den Berg), ONERA/CERT (J.Cousteix), D L R (H.U.Meier, H.P.Kreplin), DERA (M.C.P.Firmin, P.D.Smith), FFA (A.Bertelrud, J.Olsson), SAAB (E.Totland).

References

[1] Rhyming,I.L., Truong, T.V.: "Specifications for the test case: Boundary layer in a S-shaped channel (Problem T1)". Proc. of first ERCOFTAC Workshop on "Numerical simulation of unsteady flows and transition to turbulence", 1992.

[2]Schwarz, W.R., Bradshaw,P.: "Three-dimensional turbulent boundary layer in a 30 degree bend: Experiment and modelling", Stanford Univ.Thermosc.Div.Report MD-61, 1992.

[3]Pompeo, L.P.: "An experimental study of three-dimensional turbulent boundary layers", Swiss Federal Inst. of Technology, Zurich, Dissertation ETH No 9789, 1992.

[4]Anderson, S.D., Eaton,J.K.: "An experimental investigation of pressure driven three-dimensional turbulent boundary layers", Stanford Univ.Thermosc.Div.Report MD-49, 1987.

'Flack, K.A., Johnston, J.P.: "Experimental study of a detaching three-dimensional turbulent boundary layer", Proc. 1993 Conf. on "Near-wall turbulent flows", 1993.

[6]Berg, B. van den, Elsenaar, A.E.: "Measurements in a three-dimensional incompressible turbulent boundary layer in an adverse pressure gradient under infinite swept wing conditions", NLR Report TR 72092, 1972.

[7]Bradshaw, P., Pontikos, N.S.: "Measurements in the turbulent boundary layer on an infinite swept wing", J.Fluid Mech. 159, 105, 1985.

[8]Baskaran, V., Potikis, Y.G., Bradshaw, P.: "Experimental investigation of three-dimensional turbulent boundary layers on infinite swept curved wings", J.Fluid Mech. 211, 95, 1990.

[9]Driver, D.M., Hebbar, S.K.: "Experimental study of a three-dimensional, shear-driven, turbulent boundary layer using a three-dimensional Laser Doppler velocimeter", AIAA J. 25, 35, 1987.

[10]Van den Berg, B.: "A European Collaborative Investigation of the Three-Dimensional Turbulent Shear Layers of a Swept Wing", AGARD-CP-438, 1988.

[11]Firmin, M. C. P., McDonald, M.A.: "The Design of the GARTEUR Low Aspect-Ratio Wing for the Use in Validation of Shear Layer and Overall Flow Prediction Methods", AGARD FDP Symp. on 'Validation of Computational Fluid Dynamics', Lisbon, 2-5 may 1988.

[12]Gleyzes, C., Maciel, Y., Cousteix, J., Gooden, J.H.M., Reinders, W., Berg, B. van den: "Three-Dimensional Turbulent Flow around the GARTEUR Swept Wing. Selected Features". 9th Symp. on Turbulent Shear Flows, Kyoto, Japan, 1993.

[13]Gooden, J.H.M., Lent, M.L. van: "Flow gradient corrections on hot-wire measurements using an X-wire probe", 12th Symp. on Turbulence, Rolla, Missouri, NLR TP 90255, 1990.

[14]Tagawa, M., Tsuji, T., Nagano, Y.: "Evaluation of X-probe response to wire separation for wall turbulence measurements", Exp. in Fluids, 12, 1992.

[15]Maciel, Y., Gleyzes, C.: "Efficient data processing method for four-wire probe measurements in highly turbulent shear flows", ASME FEDSM97-3478, 1997.

[16]Gaudet, L., Savory, E., Toy, N.: "Calibration and use of a triangular yawmeter for surface shear stress and flow direction measurement", Second Int. Conf. on Exp. Fluid Mechanics, Turin, 1994.

[17]Barlow, R.S., Johnston, J.P.: "Roll-cell structure in a concave turbulent boundary layer", AIAA-85-293, 1985.

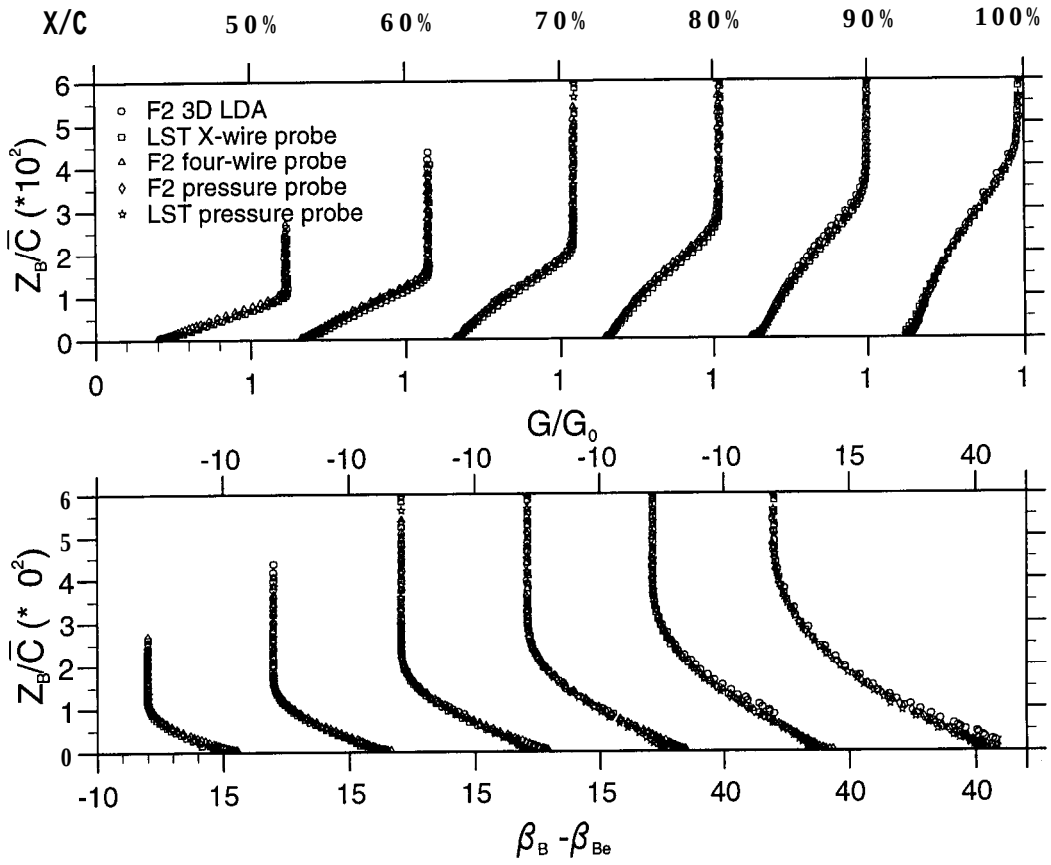

Figure 6. Evolution of mean quantities at 68% span, suction side boundary layer

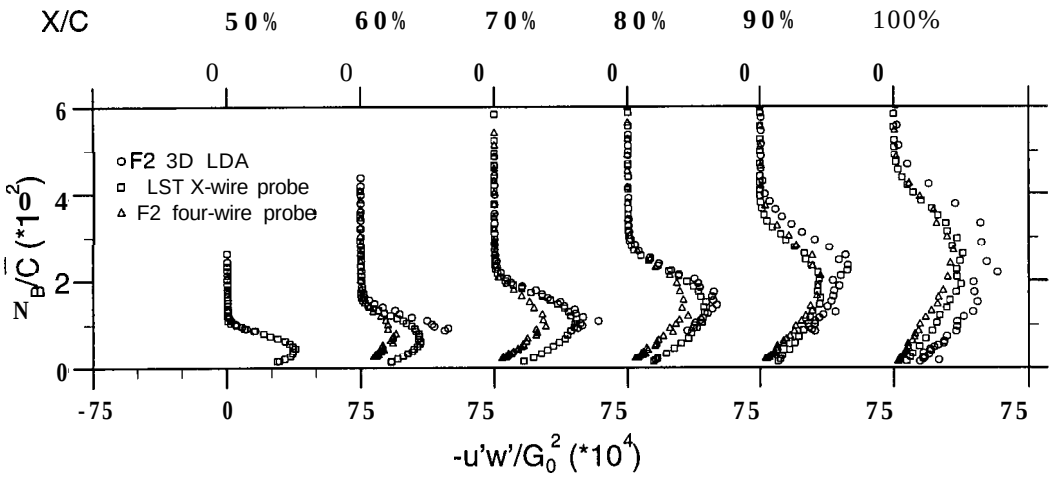

Figure 7. Evolution of turbulent shear stress at 68% span, suction side boundary layer

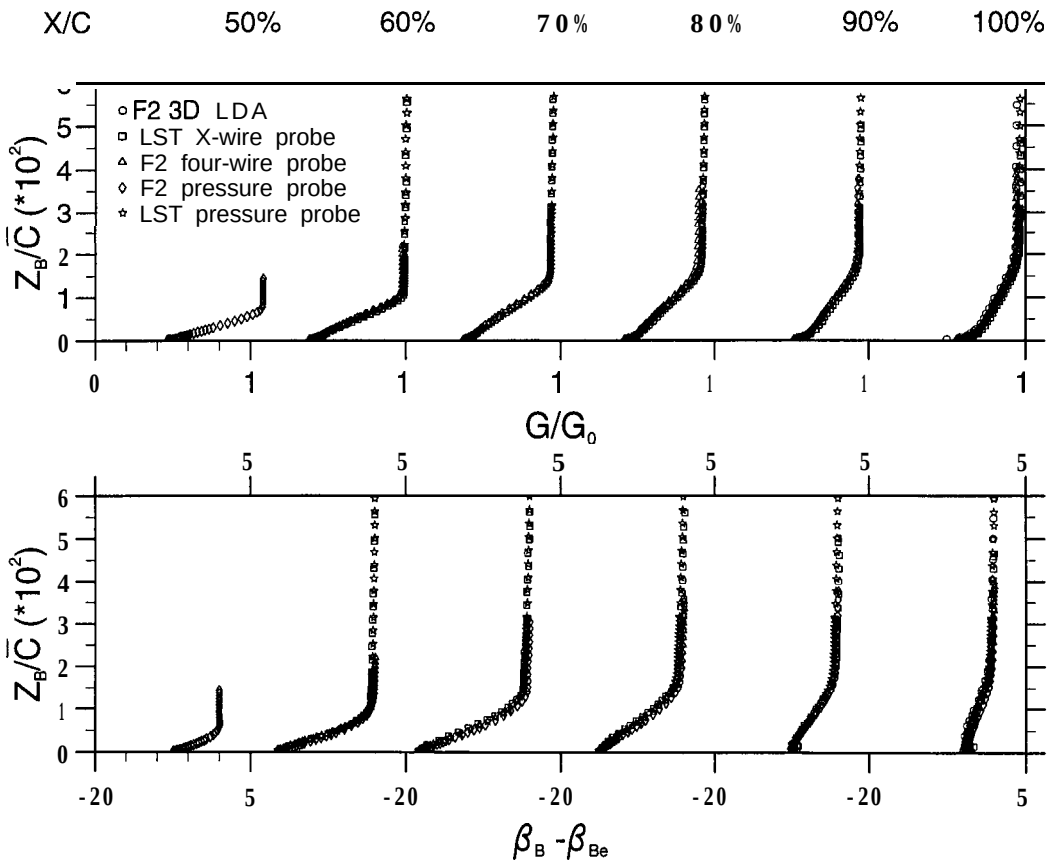

Figure 8. Evolution of mean quantities at 68% span, pressure side boundary layer

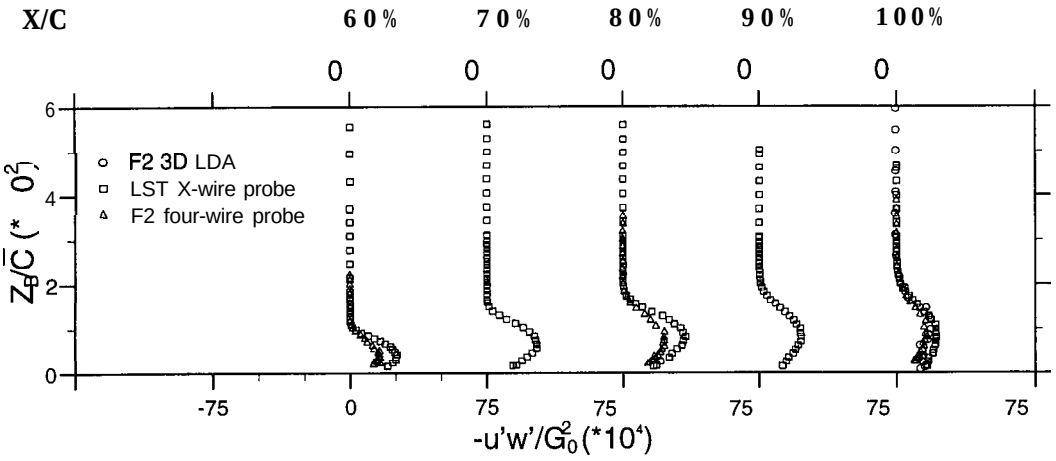

Figure 9. Evolution of turbulent shear stress at 68% span, pressure side boundary layer

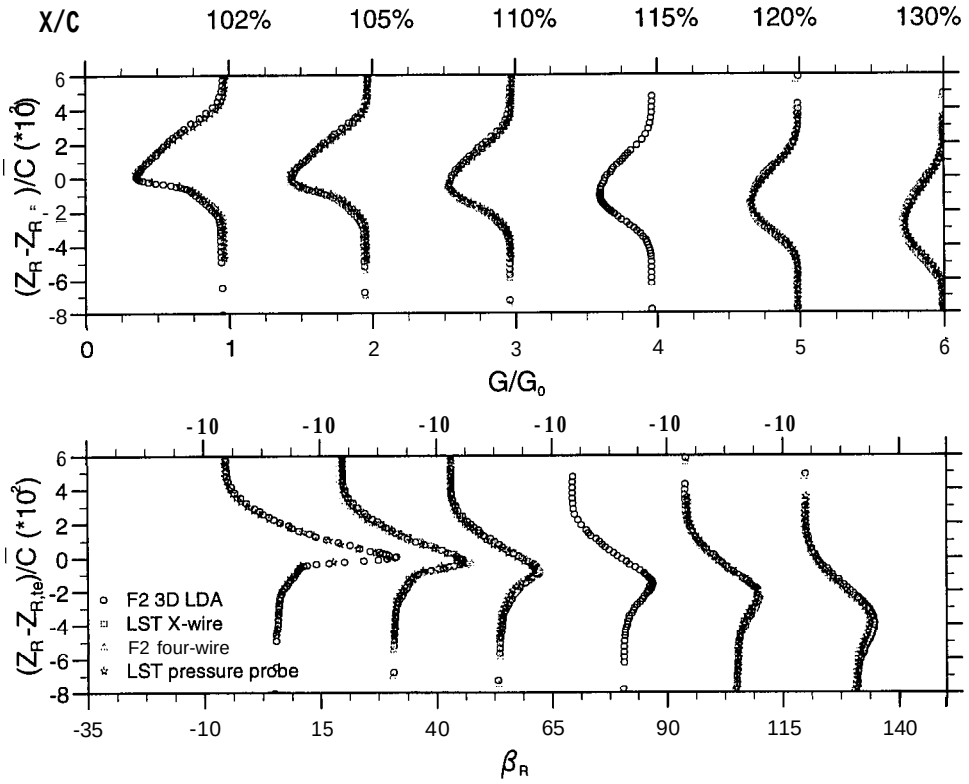

Figure 10. Evolution of mean quantities at 68% span in the wake

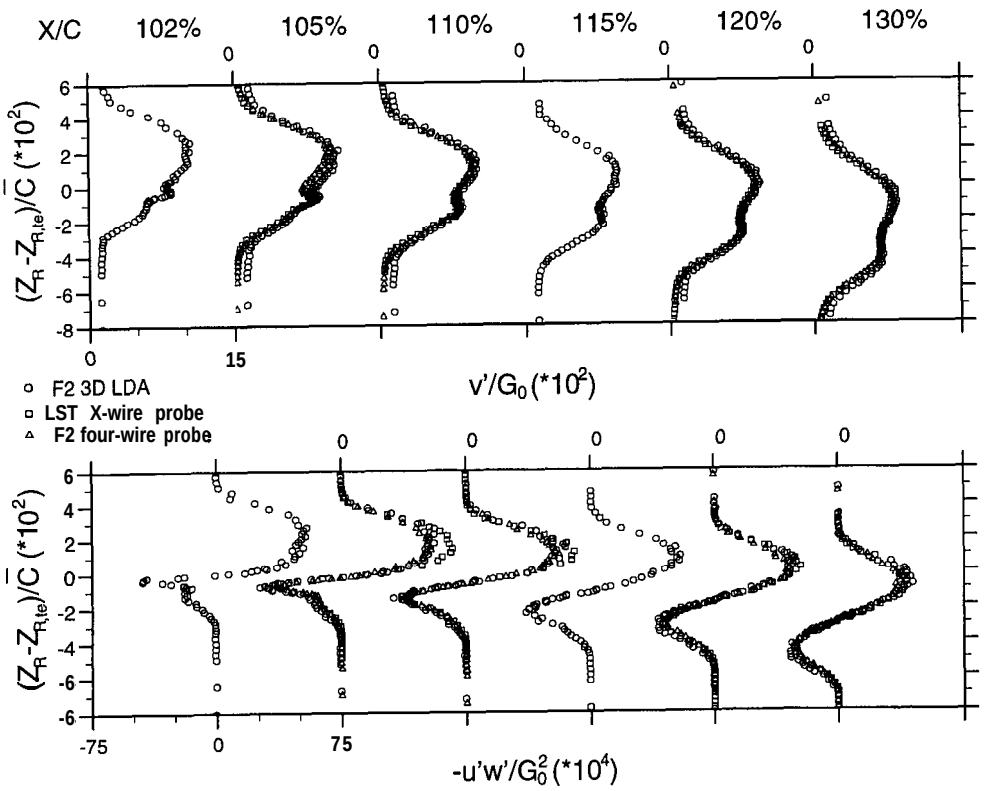

Figure 11. Evolution of turbulence characteristics at **68%** span in the wake